A real – problem simulation using fractured porous medium model[1]

JAKUB ŘÍHA, DANA ROSICKÁ & JAN ŠEMBERA
Technical University of Liberec, Studentská 2, Liberec 1, 461 17, Czech Republic
jakub.riha@tul.cz

Abstract Simulation of groundwater hydrology of a contaminated area enables to predict efficiency of a remediation intervention. We use Flow123D software, which enables to solve the task of underground water flow in heterogeneous rock, solute transport and geochemical interaction with rock. The flow model is based on mixed hybrid FEM built on combined 3D, 2D, and 1D geometry which simulates so called fractured porous medium. Solute transport is solved using operator splitting - convection is solved using FVM and geochemical interactions as a set of time-evolving mutually independent processes in various partitions of simulated area. We are going to present a model of groundwater hydrology of a real site affected by a long-term leak of chlorinated hydrocarbons. Our model was created for a purpose of remediation of contaminated soil. The model combines 3D, 2D and 1D elements of rock environment (3D porous medium, 2D fractures and 1D boreholes).
Keywords Flow123D; underground water flow; transport, Fe^0 nanoparticles

INTRODUCTION

This paper discusses the simulation of underground water flow, transport of contamination and iron nanoparticle injection on the real site. The simulated locality is called Kuřívody and it is contaminated by chlorinated hydrocarbons. On the locality, the remediation intervention is already in progress. The locality is also well explored thus suitable for the simulation.

At the beginning of this paper software used for the simulation is described. Then the basic physical laws describing the flow of underground water and the transport of its contaminants are introduced. Subsequently, the simulated locality is depicted. This is followed by the description of the simulation itself. The creation of geometry, the declaration of boundary conditions and the calibration of parameters are mentioned. Finally, the results of simulation are compared to experimental data and the fit is evaluated.

[1] This result was realized under the state subsidy of the Czech Republic within the research and development project “Advanced Remedial Technologies and Processes Centre” 1M0554 - Programme of Research Centres supported by Ministry of Education and within the research project FR-TI1/456 “Development and implementation of the tools additively modulating soil and water bioremediation” - Programme MPO-TIP supported by Ministry of Industry and Trade. This project is supported by the Technical University in Liberec within the students' project "Study of chemical processes for groundwater remediation".

SIMULATION SOFTWARE

Calculations of flow and transport were executed in the Flow123D software, which is written in the C++ programming language. It uses a mixed – hybrid finite elements method (MH-FEM) for the calculation of underground water flow. Solute transport is solved using operator splitting - convection is solved using finite volumes method (FVM) and sorption is solved numerically. To obtain a solution to the generated system of linear algebraic equations Flow123D uses external solvers like Matlab or PETSC. Geometry and mesh were created in the software called Gmsh, which is a three dimensional finite element mesh generator.

PHYSICS

The flow of a fluid through a porous medium is described by Darcy's law:

$$\vec{u} = -\mathbf{K} \cdot \vec{\nabla}\Phi,$$

where $\vec{u}$ is the filtration velocity, $\mathbf{K}$ is the hydraulic conductivity tensor and Φ is the hydraulic head.
The transport is described by the convection – diffusion equation:

$$\frac{\partial c}{\partial t} = -\nabla \cdot (\vec{v} \cdot c) + \nabla \cdot (D_m \cdot \vec{\nabla} c),$$

where c is the concentration, v is the pore velocity and D_m is the diffusion coefficient.

SIMULATION

Kuřívody locality

The Kuřívody municipality is located about 8 *km* southeast of the town called Mimoň. The area of our interest is mainly the neighbourhood of former military laundry of the Soviet Army (which used the military area in the years 1968 to 1991). Immediately after its departure, the removing of the old environmental load started. First of all, a polluted soil was mined. This was followed by pumping and decontamination of underground water. The oil based pollution did not leak into the deeper horizons and was successfully removed. Mainly in the neighbourhood of the former laundry, there is a severe massive contamination of underground water by chlorinated hydrocarbons (trichloroethylene, tetrachlorethylene, carbon tetrachloride, chloroform, dichloromethane). These are organoleptic substances dangerous to health. Therefore it is understandable that the highest priority of the remediation intervention is to prevent these substances from leaking into the sources of drinking water. The remediation intervention is performed by AQUATEST a.s., which handed us the documentation of the locality. The remediation intervention is currently still in progress, using the method of chemical reduction and oxidation, which is done by an infiltration of oxidizers or deoxidizers into a rock environment. The oxidation or the reduction takes place directly in a rock environment, rendering the pumping of contaminated water needless. In Kuřívody, potash ($KMnO_4$), lactic acid (CH_3-CHOH-COOH) and nanoiron ($nanoFe^0$) were used for this purpose.

With the aim of specification of geological and hydro geological conditions of the simulated locality some measurements were performed by Aquatest: the surface geophysics, the molecular form of elements (MFE), the well logging, the pumping

tests and the tracer tests.

Geometry of the model

Every simulation begins with the creation of geometry. First, we establish the axes. The X axis is heading from west to east. The Y axis is heading from south to north. The Z axis is orthogonal to X and Y and is used for altitude. The simulated area has a decagonal shape. The limitation of the simulated area is caused by the amount of available information from the measurements. Based on the surface geoelectrics and the MFE, the fractures were identified in the area of interest. The horizontal cut of the simulated area with marked fractures is demonstrated in Fig. 1.

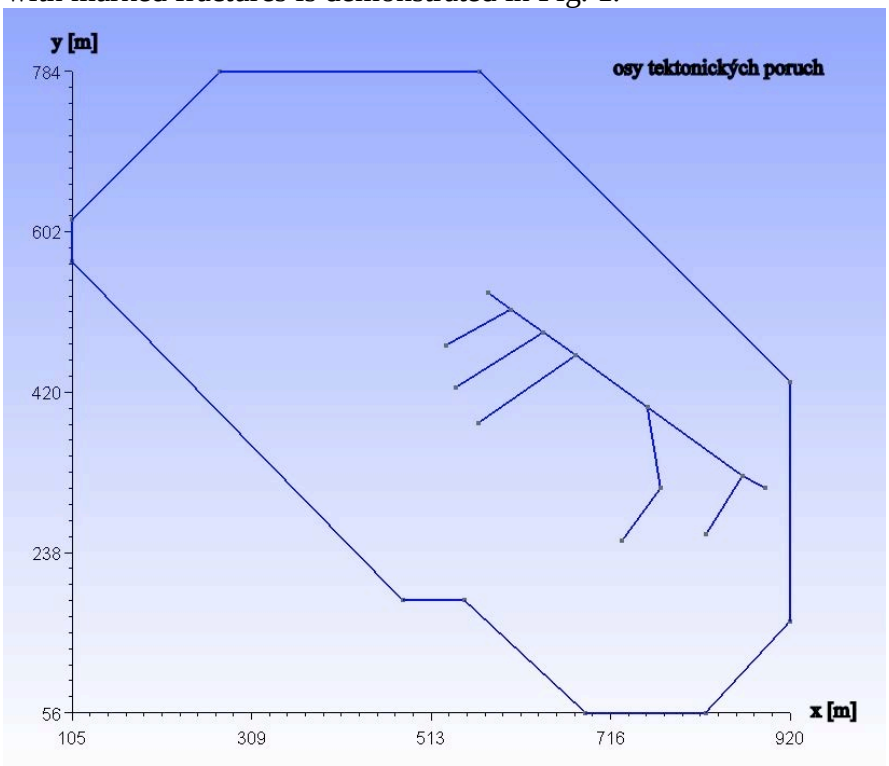

Fig. 1 Horizontal cross-section of the simulated area.

The fractures were looked for only in the proximity of the contaminated area. They probably also occur in other parts of the simulated area but, without further measurements, we cannot know where.

Based on the well logging, the pumping tests and the tracer tests, the conceptual hydro geologic model of the area of interest was put together [2]. It simplifies the multilayer collector system to three shallow aquifers and one regional Turonian collector which lies underneath them. These are separated by aquitards. The shallow aquifers are labelled (in sequence with increasing depth) A, B and C, the regional collector is labelled R and the aquitards are labelled I1, I2 and I3.

Flow123D cannot solve a problem of unsaturated flow; it calculates it as a saturated flow only with values of pressure less than zero. Since the layer R is partially unsaturated, the results of the simulation would probably be untrustworthy. This problem was solved by entering different boundary conditions for saturated and unsaturated parts of the layer R. To make this possible, the layer R was split in two (R1 and R2) at the level of geometry. R1 is the unsaturated part of the layer R, R2 is the saturated one. The layer A is also unsaturated but since it is the shallowest aquifer and its unsaturated part is rather small, it does not cause any trouble in the simulation. The

resulting eight-layer conceptual model is depicted in Fig. 2.

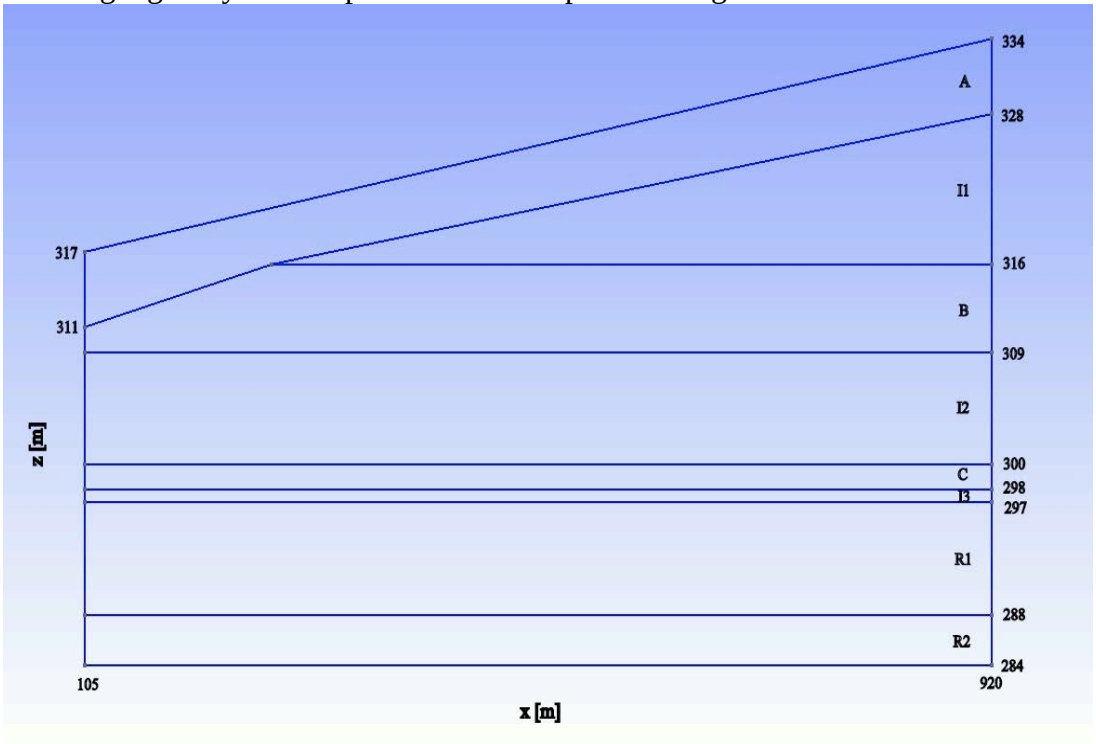

Fig. 2 Conceptual model of simulated area (vertically magnified 10x).

For the creation of geometry of more complicated layers, when the terrain had to be taken into consideration (layers A and B), we used the contour maps of tops and bottoms of these layers.

The geometry was created using the Gmsh software. The fracture is inserted only into the layer B and the layers beneath it. The layer A consists of clay, sand and weathered sandstone therefore we do not expect any fractures in it. The geometry is shown in Fig. 3 and described in Table 1.

Table 1 Parameters of geometry.

Number of points	195
Number of lines	443
Number of surfaces	321
Number of volumes	72
Number of physical groups	14

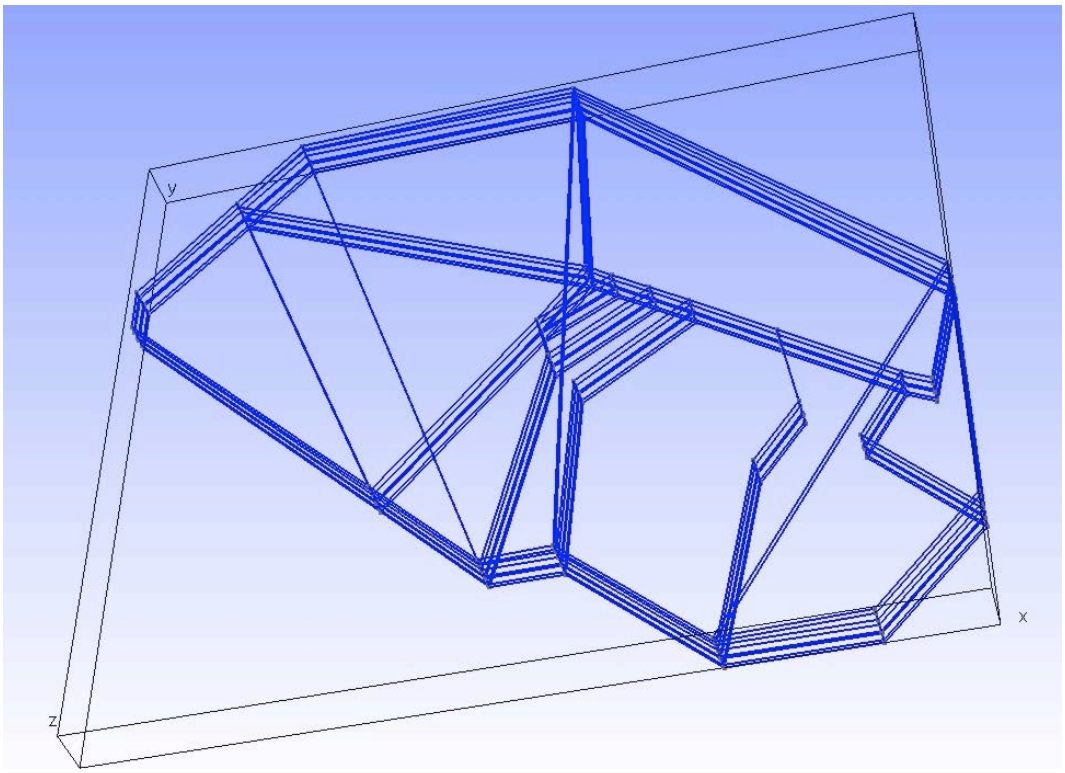

Fig. 3 Geometry of simulated area.

Subsequently, the mesh was generated in the Gmsh software. It is shown in Fig. 4 (with highlighted 2D elements ~ fracture). The mesh has 2305 nodes and 11217 elements (240 of them 2D).

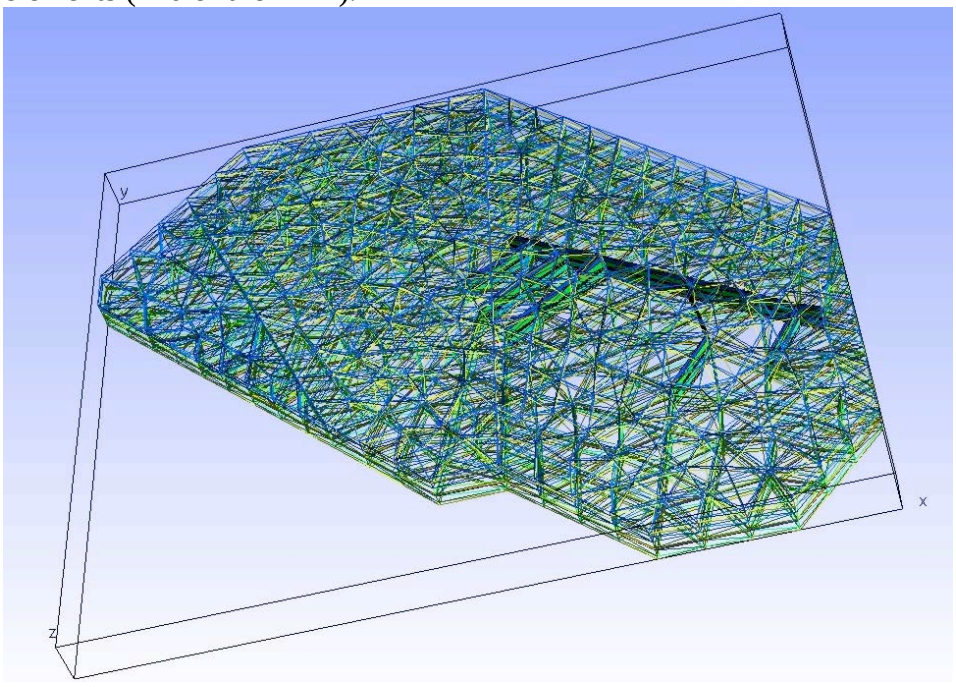

Fig. 4 Mesh of simulated area.

Simulation of flow

Throughout the simulation, we used meter as the unit of length, day as the unit of time and gram as the unit of mass.

For the declaration of boundary conditions for the underground water flow we used Dirichlet and Neumann boundary conditions. These are summarised in Table 2.

Table 2 Boundary conditions for flow.

Boundary	Boundary condition type
Edges of the layer A	Dirichlet
Edges of the layer I1	Homogeneous Neumann
Edges of the layer B	Dirichlet
Edges of the layer I2	Homogeneous Neumann
Edges of the layer C	Dirichlet
Edges of the layer I3	Homogeneous Neumann
Edges of the layer R1	Homogeneous Neumann
Edges of the layer R2	Dirichlet
Bottom of the model	Homogeneous Neumann
Top of the model	Neumann

Every layer has ten edges and on each of them, the boundary condition is declared. This was done with the aim of maximum accuracy. The values of Dirichlet boundary conditions were taken from the maps of hydroisohypses (drawn up by Aquatest). A hydroisohypse is a virtual line which connects places with the same value of the hydraulic head. The Neumann boundary condition declared on the top of the model represents the rainfall. Average yearly rainfall totals vary between 680 and 750 *mm* [2]. However, the fact, that the great portion of rainfall streams down the surface or evaporates, needs to be taken into consideration. In the area of interest, only 15% of rainfall soaks into the rock environment [1]. That gives us the resulting value of Neumann boundary condition $2.875 \cdot 10^{-4}\ m^3 \cdot m^{-2} \cdot day^{-1}$.

Since we are simulating the steady flow, the initial conditions do not need to be declared.

We used UCODE to calibrate the parameters [5]. The results of the calibration are summarized in Table 3.

Table 3 Simulation parameters and their values.

Parameter	Value
Hydraulic conductivity of the layer A	$0.3260\ m \cdot den^{-1}$
Hydraulic conductivity of the layer I1	$1.7 \cdot 10^{-3}\ m \cdot den^{-1}$
Hydraulic conductivity of the layer B	$0.1714\ m \cdot den^{-1}$
Hydraulic conductivity of the layer I2	$7 \cdot 10^{-8}\ m \cdot den^{-1}$
Hydraulic conductivity of the layer C	$0.1555\ m \cdot den^{-1}$
Hydraulic conductivity of the layer I3	$2 \cdot 10^{-7}\ m \cdot den^{-1}$
Hydraulic conductivity of the layer R1	$0.031\ m \cdot den^{-1}$
Hydraulic conductivity of the layer R2	$0.031\ m \cdot den^{-1}$
Hydraulic conductivity of the fracture	$1 \cdot 10^{-8}\ m \cdot den^{-1}$
Porosity	0.2

Hydraulic conductivities of layers A, B, C and R listed in Table 3 are the horizontal ones. The values of the vertical ones are ten times lower. The values of the parameters are physically realistic, only the value of hydraulic conductivity of layer R is about ten times lower than we would expect. The simulation is not very sensitive to this parameter hence its value cannot be well calibrated.

The comparison between the simulated values of hydraulic heads in the observation points and the measured ones is listed in Table 4.

The correspondence between the simulated values and the measured ones is good. The value of objective function converged to 26.281, ideally it should be zero. With the increasing number of parameters the difference between the model and the reality diminishes (the value of objective function decreases), however we cannot use parameters which are not supported with observations. The more parameters we calibrate, the less reliable is their estimation. This fact is taken into account by the calculated error variance (CEV) statistic. In our case its value is 2.6281. The square root of CEV is called standard error of regression (STD ERR) and in our case it equals 1.6211. Both these statistics should be ideally equal to one. When they are not, it could mean one of two things. Either the weights of observations are too big or the simulation is inaccurate. In our case, the error of model could be up to 1.6211 times greater than the measurement error.

Table 4 Measured and simulated values of hydraulic heads in the observation points.

Observation	**X (*m*)**	**Y (*m*)**	**Z (*m*)**	**Measured value (*m*)**	**Simulated value (*m*)**
A1	206.8	524.1	319.7	319.52	317.687
A2	363	410.1	322.9	318.62	319.937
A3	652	247.7	327.6	328.52	326.567
A4	844.37	349.67	331.49	331.72	331.207
A5	751.27	158.54	328.91	327.76	328.307
B1	556.4	264.4	309	321.78	322.992
B2	758	403	309	327.12	327.513
B3	767	172.1	309	324.48	325.736
B4	698.25	104.75	309	323.81	325.630
B5	312.2	447.75	309	315.34	319.323
C1	566	385	298	320.66	321.134
C2	626.43	271.92	298	321.62	322.028
C3	676.98	407.82	298	321.16	321.383
C4	718.75	202.25	298	322.91	322.640
R1	262.94	451.57	284	288.71	288.111
R2	602.21	324.18	284	288.47	288.184
R3	729	251	284	288.23	288.011

Fig. 5 shows the graph of weighted residuals of observations.

The closer are the values of weighted residuals to zero, the better. Ideally, the number of weighted residuals lesser than zero should be equal to the number of the ones greater than zero. In our case seven residuals are greater than zero a ten residuals are lesser than zero.

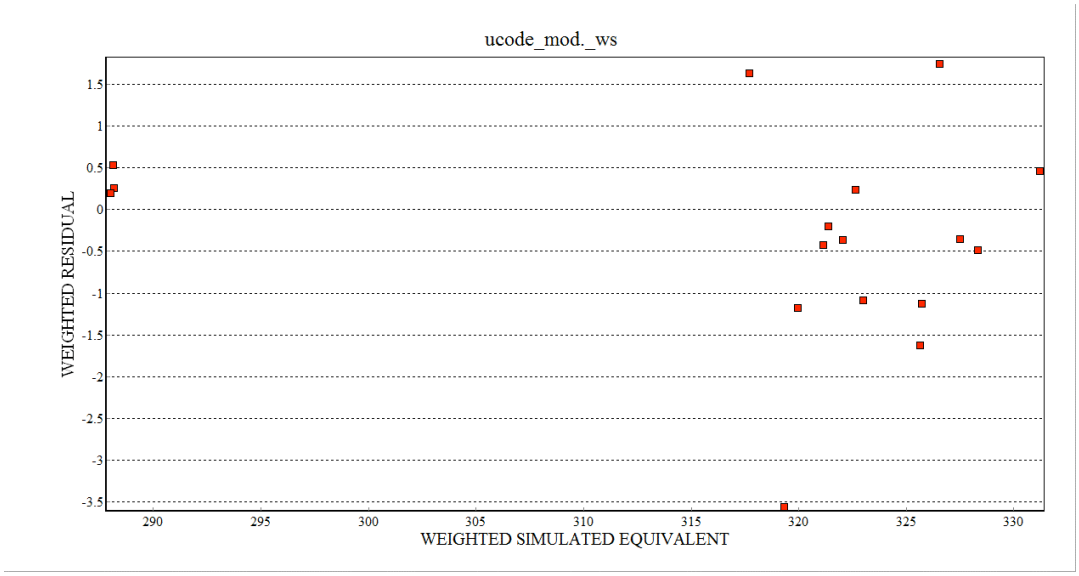

Fig. 5 Weighted residuals of observations.

The greatest deviations between the simulated values and the measured ones are in the western part of the layer B where there it is adjacent to the layer A (there is no aquitard between them). This inaccuracy of simulation is caused by the fact that the hydraulic conductivity of every layer is uniform in their entire volume (layers are homogenous). That is in actuality quite unlikely. The fit of the model could be improved by splitting the layers into the zones with unequal values of hydraulic conductivity. This would have to be done at the level of geometry, which would be arduous.

Figs. 6 – 9 show the comparison of hydroisohypse maps of layers A, B, C and R (with highlighted observations used for calibration) with simulated hydraulic heads of the same layers.

The layer R is poorly explored (only three boreholes situated on the almost straight line). Any interpretation in the layer R in both forms (hydroisohypse map and model output) is not conclusive. The gradient of hydraulic head in layer R is so small that the model output is quite uninteresting. It would probably be for the best not to simulate this layer at all.

The correspondence between the model output and the maps of hydroisohypses is relatively good. It could be improved by methods mentioned above. The closed path in the hydroisohypse map of layer B is caused by the programme interpretation of measurements, it has no cause and there would be no point in trying to replicate it in the model output.

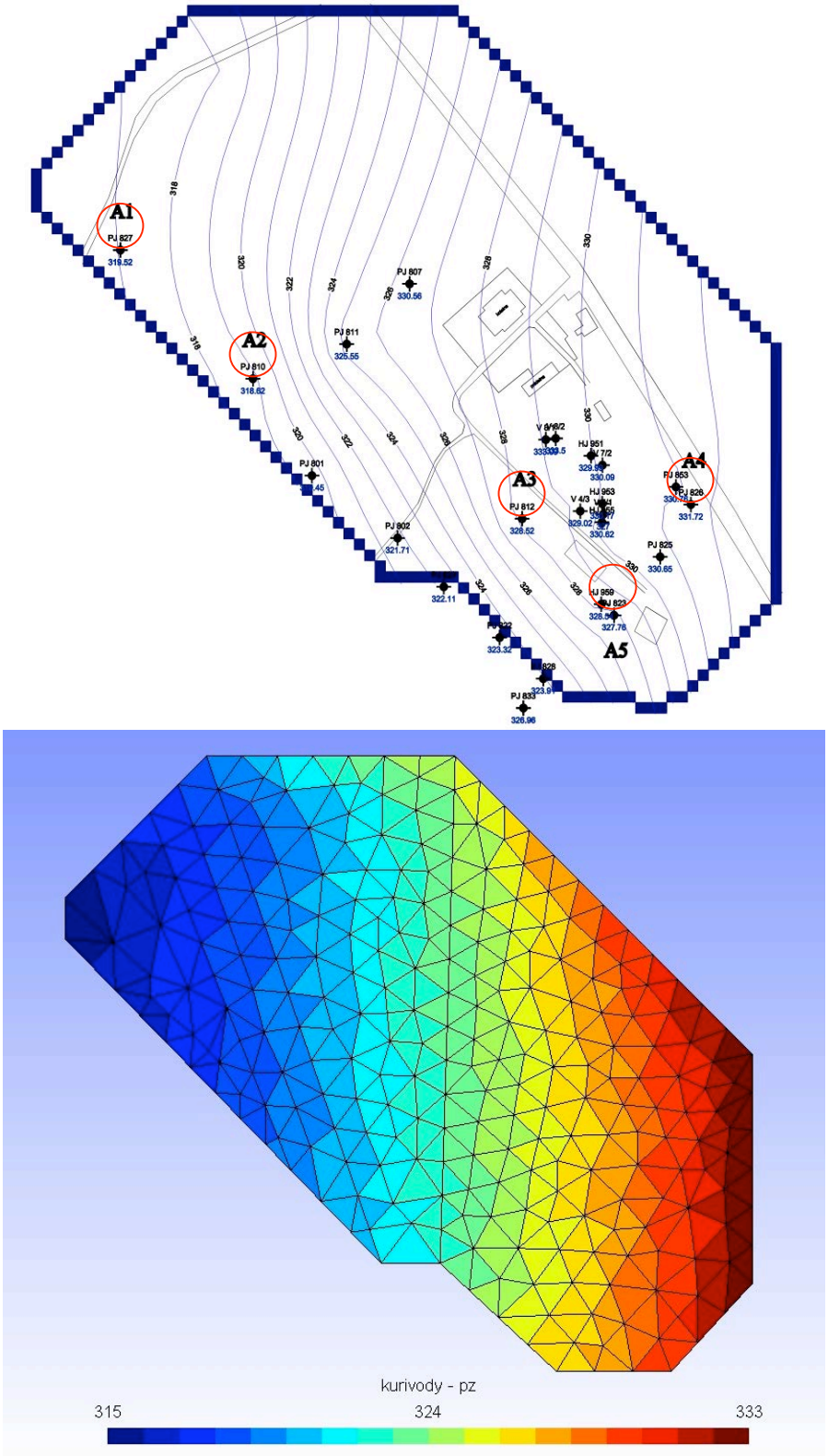

Fig. 6 Comparison of measured hydraulic heads of layer A with the simulated ones.

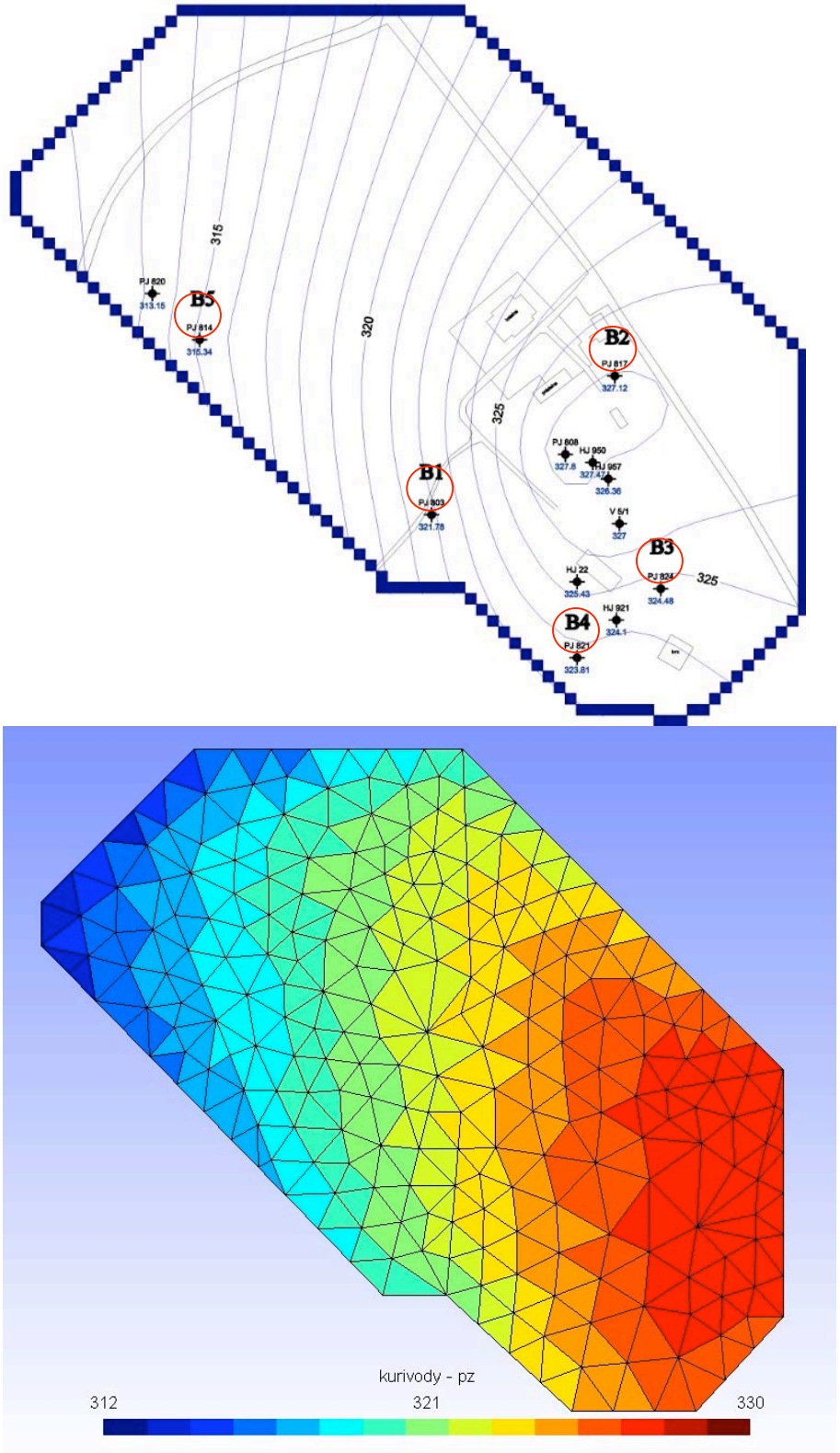

Fig. 7 Comparison of measured hydraulic heads of layer B with the simulated ones.

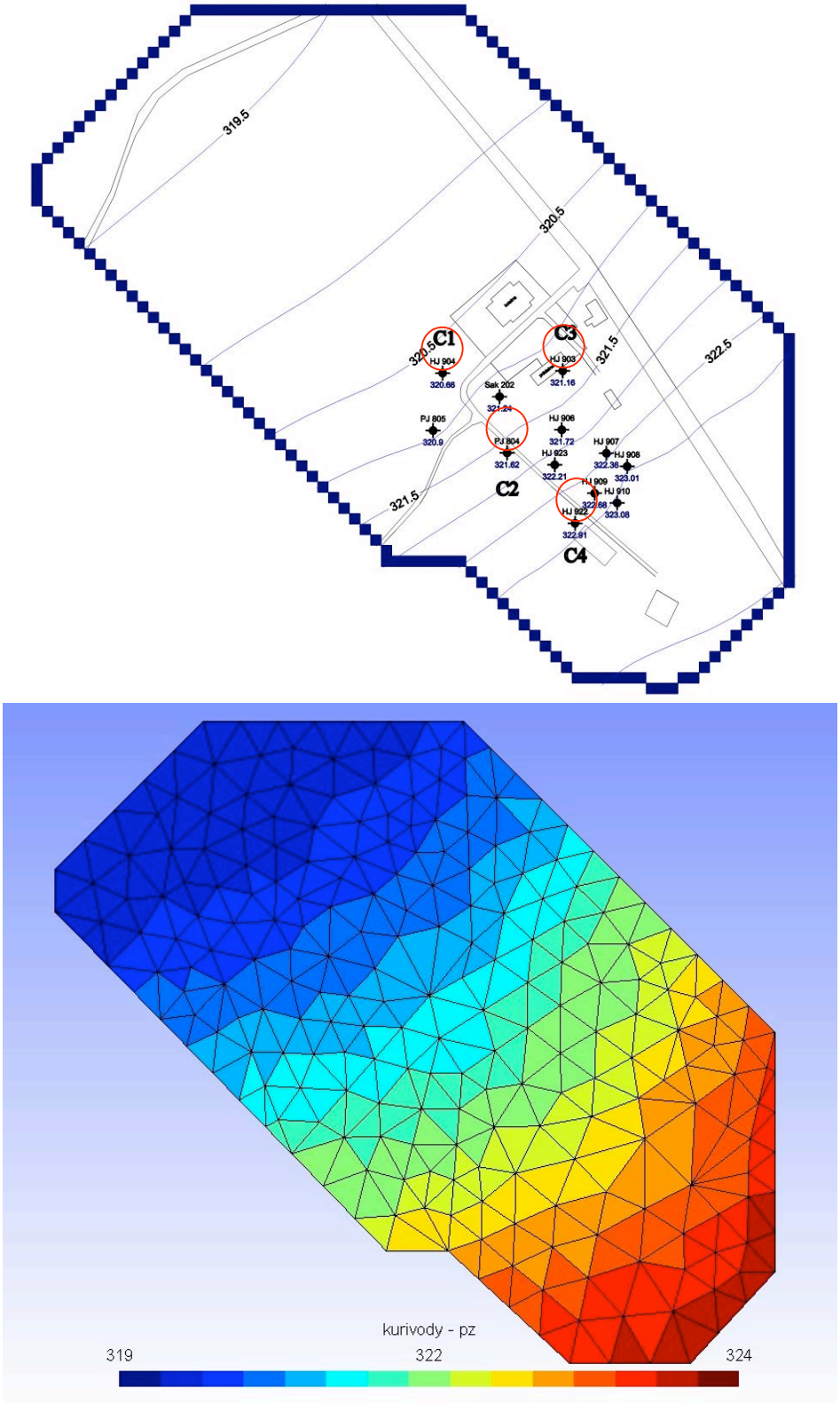

Fig. 8 Comparison of measured hydraulic heads of layer C with the simulated ones.

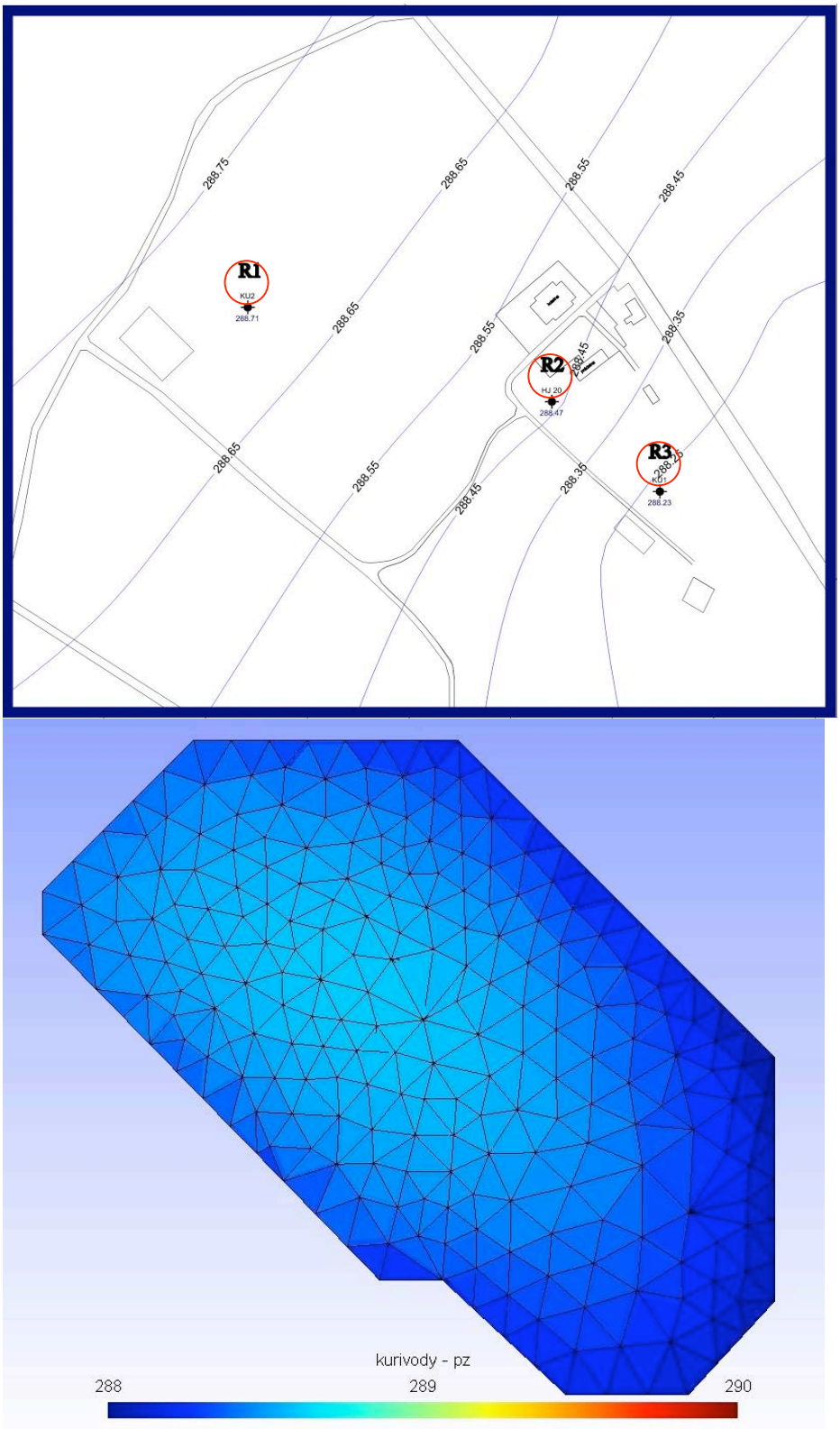

Fig. 9 Comparison of measured hydraulic heads of layer R with the simulated ones.

Fig. 10 shows the vectors of filtration velocity in the cut-out of the vertical cross-section of the simulated area.

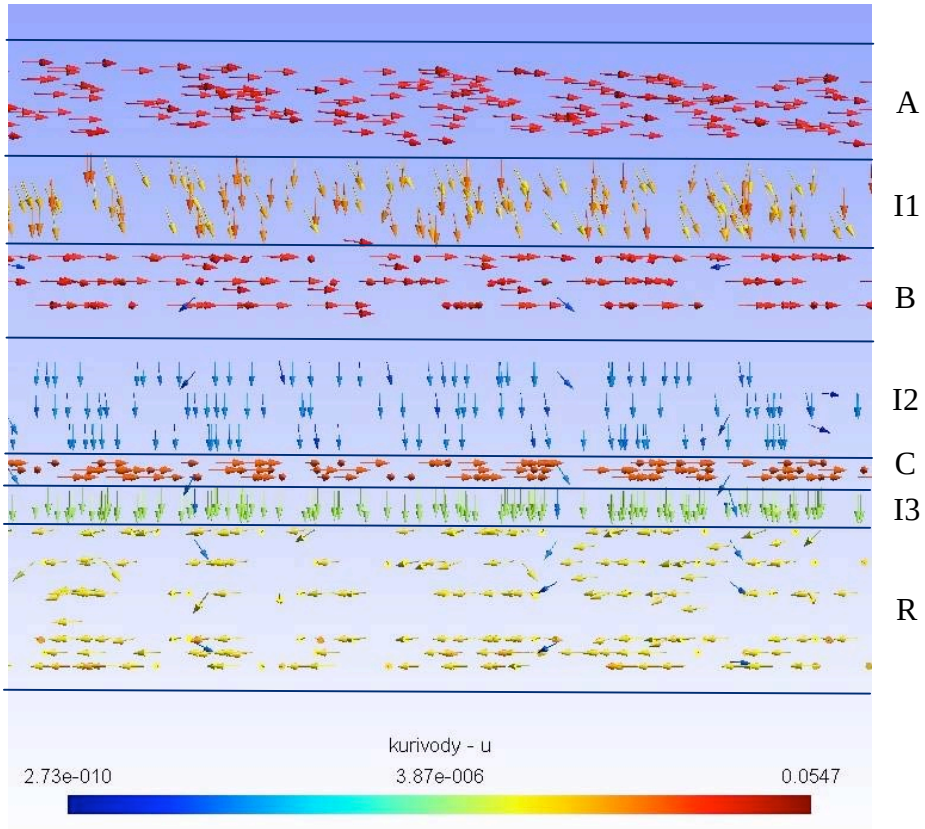

Fig. 10 Vectors of filtration velocity in the vertical cross-section of the simulated area.

In agreement with presumptions, the direction of flow in the layer R is opposite to the direction of flow in other layers.

Table 5 summarizes the water budget of aquifers. Flow123D can only compute a flux across the boundaries of model. Possible flux between layers has to be calculated manually.

Table 5 Water budget.

Boundary	**Flux ($m^3 \cdot den^{-1}$)**
Rainfall	-10.7576
Edges of the layer A	-164.382
Edges of the layer B	175.14
Edges of the layer C	-2.47319
Edges of the layer R	2.462

Values less than zero indicate the influx, the ones greater than zero indicate the outflow. Values of flux might seem big but we need to keep in mind that the simulated area is quite large (its volume is 3 183 420 m^3). As we can see from the Table 5, the greatest flux is between layers A and B. Fluxes among other layers are strongly limited by low hydraulic conductivity of layers I2 and I3.

Simulation of transport

This chapter deals with the transport of contamination in the simulated area. The bases of the simulation of transport were the maps of contamination plums of layers A, B

and C (drawn up by Aquatest) which represent the state of the area in 2004. Other available information was the anticipated remaining amount of chlorinated hydrocarbons in the rock environment (c. 1350 *kg* [2]).

The simulation of transport was based on the calibrated model of flow. The beginning of the simulation was set to 25 years before the time when the documentation was made. That is probably the time when the contamination of the area started. The aim was to replicate the current shape of contamination clouds.

The boundary condition of constant concentration was declared on the source element. Then, the simulation was started, this time without retardation. The value of boundary condition was being altered in order to match the anticipated amount of contamination (1350 *kg*). A program which computes the total amount of substance in simulated area was written for this purpose. The final value of boundary condition was 55000 $g \cdot m^{-3}$.

The result of simulation is extremely different from observed reality. The biggest difference was the fact that the real contamination penetrated into lower layers and was not spreading only in layer A as it was simulated. The real contaminating substance is not fully dissolved in the underground water. It would have to be simulated as a multiphase flow but Flow123D is unable to do so. Chlorinated hydrocarbons have greater density than water (e.g. the density of tetrachlorethylene is 1622 $kg \cdot m^{-3}$) which enables them to penetrate to the deeper layers. Such a penetration can be eased by poorly equipped boreholes.

These findings limited our effort to an attempt to replicate the shape of the contamination plum in the layer A. The rate of spread of contamination can be influenced by alternation of the retardation coefficient. In Flow123D, the retardation is realized by the sorption. We have chosen to use the linear sorption. The best fit was achieved, while keeping just one source element, with the distribution coefficient $k_D = 1.5$.

Fig. 11 shows the actual shape of contamination plum in the layer A.

Fig. 12 shows the simulated shape of contamination plum in the layer A (with highlighted source element).

It is obvious that the correspondence between the model and the reality is quite poor. This has two basic causes:

1. Flow123D cannot compute diffusion. The presence of numerical dispersion cannot compensate this limitation.

2. The simulated direction of flow (east to west) is slightly different than the actual one (southeast to northwest). That is why the contamination cloud is elongated in different direction.

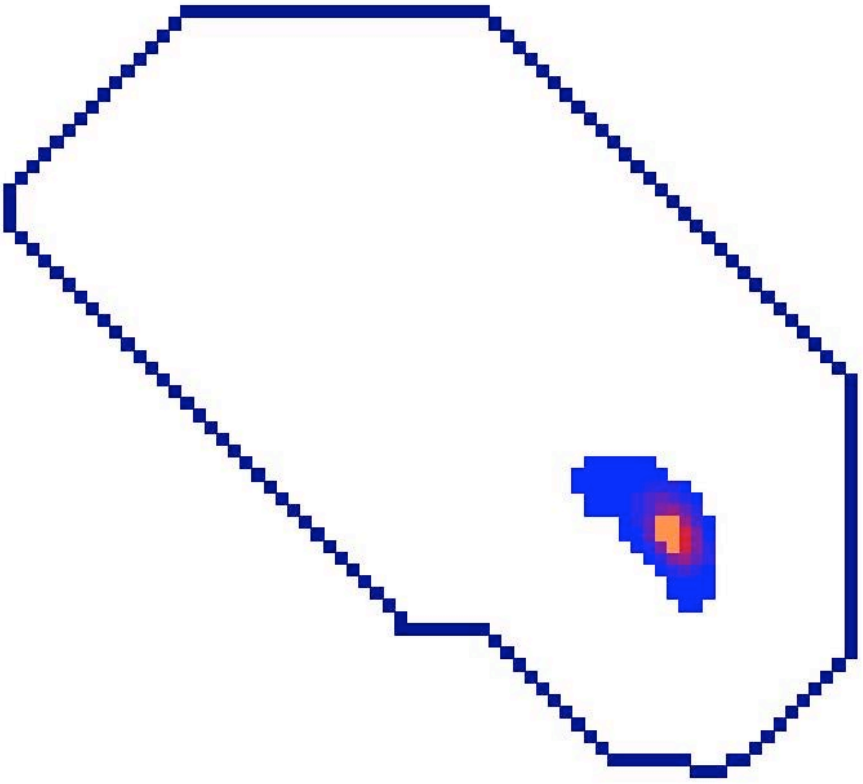

Fig. 11 Actual shape of contamination plum in the layer A.

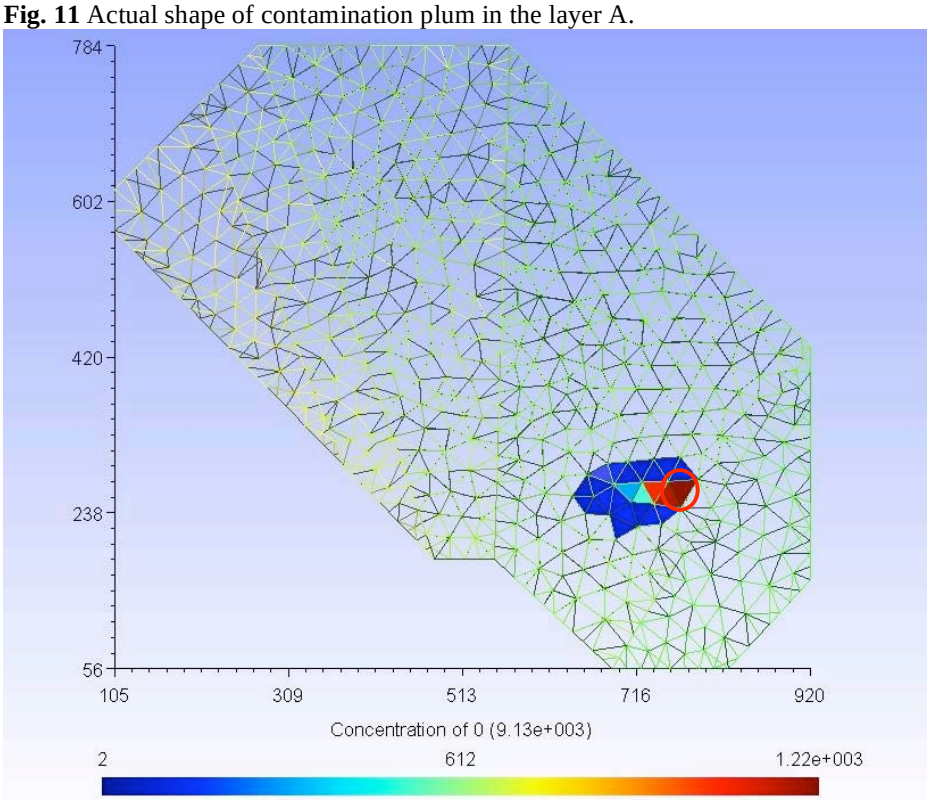

Fig. 12 Simulated shape of contamination plum in the layer A.

Simulation of iron nanoparticle injection

In situ, the iron nanoparticle injection was actually performed and documented by Aquatest. This documentation [2] served as a basis for the simulation.

Our original intention was to simulate the nanoparticle injection within the whole simulated area. This intention was abandoned because the requirements for the fineness of the mesh could not be met. The monitoring boreholes used for the detection of concentration of nanoiron are only several meters away from the application borehole therefore the size of elements edges could not be much greater than one meter. There were two possible solutions to this problem. We could locally refine the mesh but that would require changes in geometry because the density of nodes can be influenced only in vicinity of points which are explicitly defined in the geometry. In the current geometry, there is no such point in the vicinity of the application borehole. The other possible solution, which we have chosen, was to create a new geometry. It represents the cut of original geometry. It includes the application borehole and its closest vicinity (about 5 meters to each direction). The coordinates of the application and the monitoring borehole and their parameters are listed in Table 6.

Table 6 Coordinates and parameters of used boreholes.

	PW-3	**MW-2**
Type	Application	Monitoring
X (*m*)	576.8	573.4
Y (*m*)	295.7	295.6
Depth (*m*)	15	15
Diameter (*m*)	0.16	0.16

The distance between the application borehole and the monitoring one is about three meters. Vertically, the new geometry is limited to layers A, I1 and B. We could have done that, without dramatically harming the accuracy of the simulation, because the flux between layers B and C is minimal (see Table 5). The new geometry is shown in Fig. 13.

The mesh was generated in Gmsh. It has 986 nodes and 4702 elements (all of them 3D).

The next step was to declare the boundary conditions. These are listed in Table 7.

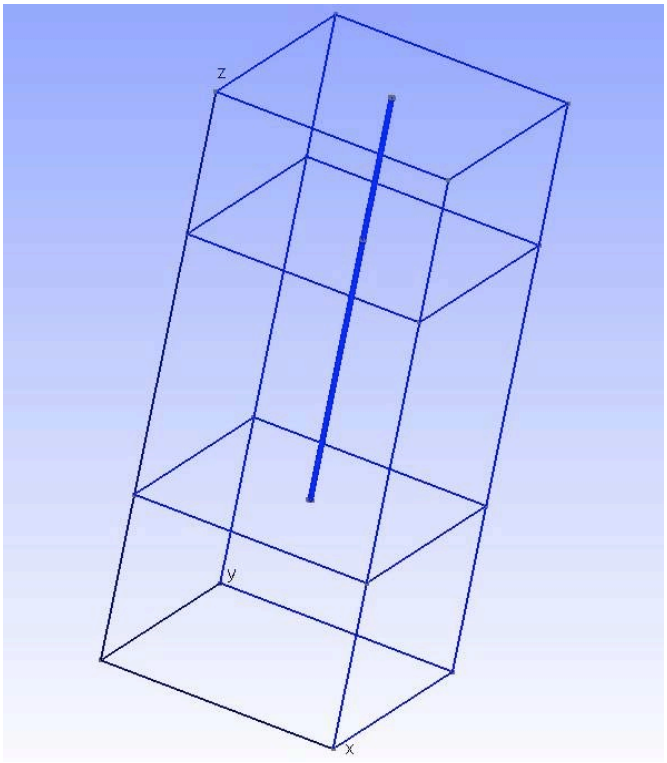

Fig. 13 Geometry for nanoparticle injection.

Table 7 Boundary conditions for flow.

Boundary	Boundary condition type
Edges of the layer A	Dirichlet
Edges of the layer I1	Homogeneous Neumann
Edges of the layer B	Dirichlet
Bottom of the model	Homogeneous Neumann
Top of the model	Neumann
Sides of the borehole	Homogeneous Neumann
Bottom of the borehole	Neumann

The Dirichlet boundary conditions of layers A and B were declared on the basis of the model of flow of the whole simulated area. The Neumann boundary condition on the top of model represents the rainfall. Its value is the same as the one in the original simulation. We presume a well equipped borehole, i.e. its sides are impermeable. The value of the boundary condition on the bottom of borehole is in time of no injection identical with the one on the top of the model.

The simulation of injection was performed as follows:

1. A Boundary condition for transport was declared on the bottom of the borehole. It was the condition of constant concentration. Its value was 1000000 $g \cdot m^{-3}$.

2. The simulation of transport was started. The stop time of simulation was set 7.5 hours [2].

3. The value of Neumann boundary condition on the bottom of the borehole was being altered so the total amount of injected nanoiron would reach 22 kg. The total amount of nanoiron in the simulated area was in each step calculated by the program written for this purpose. With the value of boundary condition equal to $7\ m^3 \cdot m^{-2} \cdot day^{-1}$ the total amount of injected nanoiron was 22627 g which is sufficiently close to the requested value.

4. Values of concentrations in elements saved in the Flow123D output file were, using a simple program, converted to transport initial conditions file. With these initial

conditions, the simulation was restarted this time with the normal boundary conditions (just rainfall on the bottom of the borehole).

The only remaining thing was to find out what value of retardation coefficient corresponds with the expected rate of spread of iron nanoparticles (1 meter per month). We found, using a program written for this purpose, an element closest to the coordinates of the bottom of the monitoring borehole. The same program then listed values of concentrations in that element in each time step. Fig. 14 shows the development of values of concentration in the monitoring element (with no retardation).

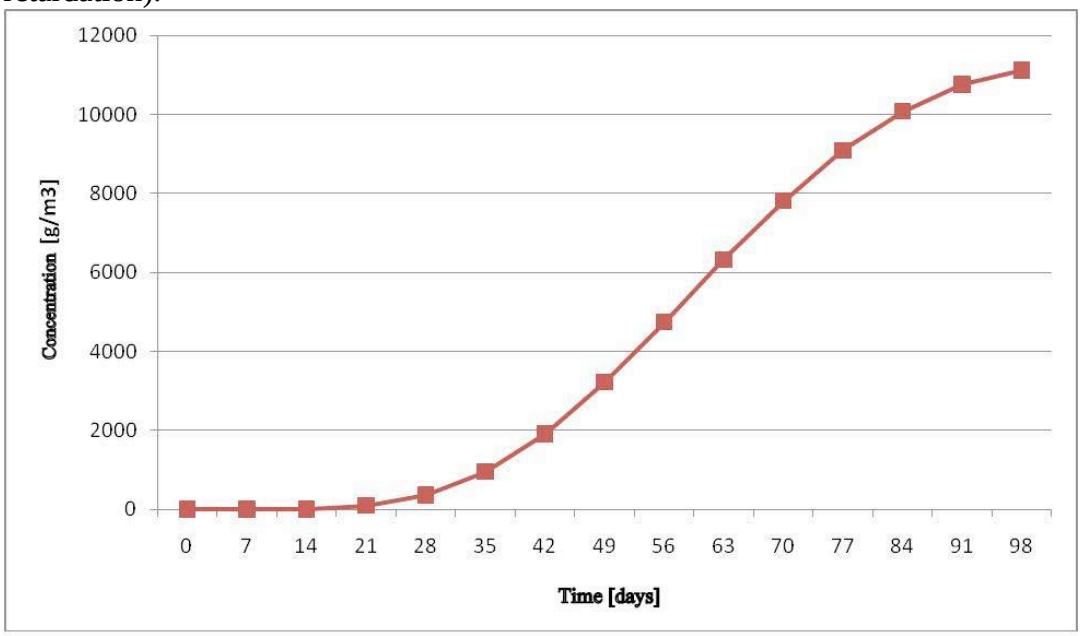

Fig. 14 Concentration in the monitoring element (no retardation).

The retardation was realised by the linear sorption. Its value is determined by the value of distribution coefficient k_D. Fig. 15 shows the development of concentration in the monitoring element for various values of retardation.

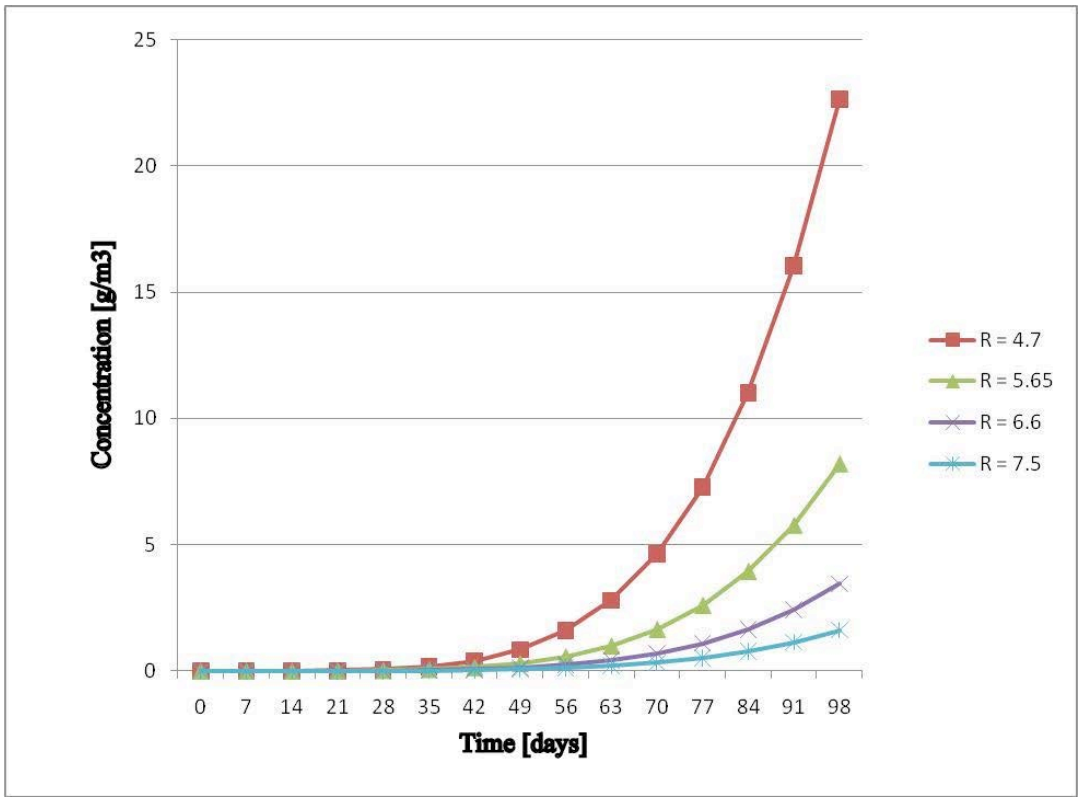

Fig. 15 Concentration in the monitoring element for the various values of retardation.

The goal was for the nanoiron to reach the monitoring element in three months. This was accomplished with the value of retardation coefficient equal to 7.5 (the concentration in the monitoring element was lesser than 1 $g \cdot m^{-3}$ till 91st day and greater than 1 $g \cdot m^{-3}$ after 91st day). This value corresponds to the value of distribution coefficient $k_D = 3.5$ ($K_D = 3.5\ cm^3 \cdot g^{-1}$, $\rho = 1\ g \cdot cm^{-3}$). Distribution coefficients ascertained from the column experiments described in [3] (second column of table) and [4] (third column of table) are listed in Table 8.

Table 8 Distribution coefficients from column experiments.

	$K_D\ [cm^3 \cdot g^{-1}]$	$K_D\ [cm^3 \cdot g^{-1}]$
Fraction I (finest)	0.032	0
Fraction II	1.76	12
Fraction III (coarsest)	22.7	35
Avarage	4.8	12.55

Correspondence between the distribution coefficient used in the simulation and the ones from the column experiments is good. The difference can be explained by the dissimilarity of rock environment where the transport took place.

The monitoring borehole was in the direction of underground flow from the application borehole. This means that the advection was greater than the diffusion and the inability of Flow123D to compute diffusion did not show.

CONCLUSIONS

We have used Flow123D to successfully simulate the underground water flow on the real site. The model was calibrated using UCODE. However, we have failed to simulate the transport of contamination. This was caused by the inability of Flow 123D to compute multiphase flow and diffusion. Finally, we have succeeded in simulating the iron nanoparticle injection but it would be much harder, or maybe even impossible, if the monitoring borehole were not in direction of underground flow from the application one.

Flow123D seems to be a quality software with great potential which will be, after implementation of some missing functionalities, usable for wide spectra of underground flow and transport problems.

REFERENCES

[1] Krásný, J., Daňková, H., Hanzel, V., Kněžek, M., Matuška, M., Šuba, J.: Mapa odtoku podzemní vody ČSSR 1:1000000 (Map of discharge of underground water in ČSSR). Czech Hydrometeorological Institute, Praha, 1981.

[2] Kvapil, P.: Documentation to the chosen pilot experiment, technical report, Aquatest, 2004.

[3] Nosek, J.: Laboratorní výzkum a modelování transportních vlastností nanoželeza (Laboratory research and modelling of nanoiron transport properties), dissertation thesis FM TUL, 2009.

[4] Pelikánová, D.: Model agregace nanočástic (Nanoparticle aggregation model), diploma thesis NTI TUL, 2008.

[5] Poeter, E. P., Hill, M. C., Banta, E. R., Mehl, Steffen, and Christensen, Steen, 2005, UCODE_2005 and Six Other Computer Codes for Universal Sensitivity Analysis, Calibration, and Uncertainty Evaluation: U. S. Geological Survey Techniques and Methods 6-A11, 283p.